JOURNAL OF MATERIALS SCIENCE 23 (1988) 3206–3213

Fracture toughness and fatigue crack growth behaviour of an Al_2O_3–SiC composite

A. A. MORRONE, S. R. NUTT, S. SURESH
Division of Engineering, Brown University, Providence, Rhode Island 02912, USA

The fracture toughness and fatigue crack growth characteristics of an Al_2O_3–SiC whisker composite were investigated. Quasi static fracture experiments were conducted on double edge-notched tension specimens and on four-point bend specimens containing a through-thickness Mode I crack which was introduced under uniaxial cyclic compression. The toughness results obtained using this procedure are more reproducible than those derived from the indentation technique and the notched bend bar method. The fracture toughness of the composite is about 60% higher than that of the unreinforced matrix material. Crack growth characteristics at room temperature were also investigated in notched plates of Al_2O_3–SiC subjected to fully compressive far-field cyclic loads. In the presence of a stress concentrator, this composite is found to be highly susceptible to fatigue crack growth under cyclic compressive loads.

1. Introduction

Much research effort has been directed successfully towards improving the fracture toughness of ceramics, increasing their potential for structural applications in severe environments. In particular, SiC whisker-reinforced Al_2O_3, which is currently being manufactured for cutting tool applications, has twice the toughness of monolithic Al_2O_3 [1–4]. However, there are inconsistencies when comparing toughness values for a given ceramic because the fracture toughness measurements for ceramics and composites have not been standardized. Furthermore, potential applications for these materials are likely to involve cyclic loads, particularly in compression because brittle solids are much stronger in compression than in tension. However, little is known about the resistance of ceramic composites to fracture under cyclic loads.

The present work was undertaken with the objective of investigating the fracture toughness of Al_2O_3–SiC composites. The approach was to develop a procedure introducing a Mode I fatigue pre-crack (as in the case of metals) prior to the fracture toughness testing of the ceramic composite and to compare with existing techniques for measuring toughness. Because ceramics and composites are often employed in compression-dominated applications, this work also focused on investigating the resistance of Al_2O_3–SiC to fatigue under uniaxial cyclic compression. To achieve the primary objective, single and double edge-notched specimens were pre-cracked in compression fatigue and fracture toughness was measured in four-point bend and in tension, respectively. For comparison purposes, toughness was also measured using the indentation method and the single edge-notched bend specimen without a pre-crack. The fatigue studies involved measurements of crack initiation and growth under uniaxial cyclic compression on specimens containing different notch geometries.

Different techniques and specimen geometries are being used for toughness testing, on the basis of approaches different from those established for metals. The toughness testing methods most commonly employed include the single edge-notched bend test [5, 6], the chevron V-notched bar or short rod tests [7, 8], the bridge compression method [9, 10] and the indentation technique [11, 12]. Except for the bridge compression method, these techniques share the advantage that they do not require the introduction of a sharp through-thickness crack in the specimen prior to fracture testing. The development of fracture test methods for ceramics using these techniques has been the subject of recent studies (e.g. [5–14]). Introducing and controlling a through-thickness crack in brittle solids by conventional methods is problematic because, unlike metals, they fail catastrophically with little or no stable crack growth under tension at room temperature. Recently, Suresh and co-workers [15–17] suggested a technique which can potentially enable the measurement of the fracture properties of brittle solids as is done in metals. Their technique consists of introducing a through-thickness crack in notched specimens by means of compressive cyclic loads applied normal to the plane of the notch. The fatigue crack starts at the notch and propagates perpendicular to the loading direction at progressively decreasing rates until it arrests. A tensile residual stress zone which developed at the notch tip upon removal of the far-field compressive load is responsible for crack growth, although the micromechanism of failure differs among different materials [16]. The crack ceases to grow beyond the residual tensile "damage" zone as it enters material strained elastically in compression, thus resulting in a self-arresting stable crack growth. Moreover, the damage left at the crack tip of the arrested crack is small and appears to have negligible effect on subsequent measurements of fracture tough-

0022–2461/88 $03.00 + .12

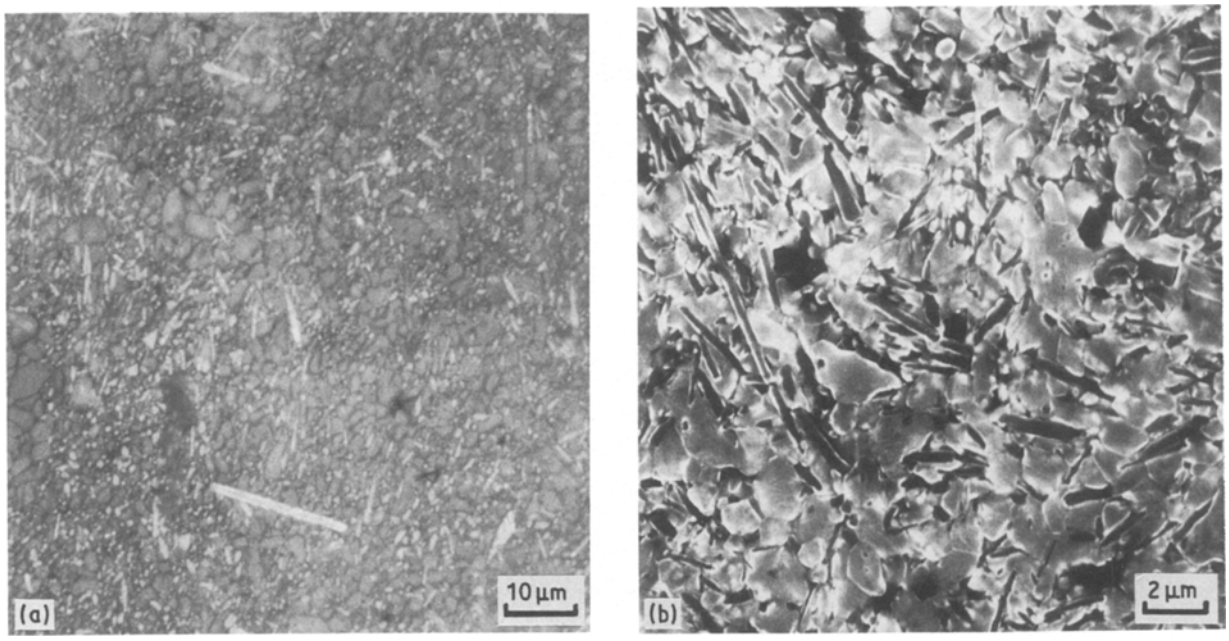

Figure 1 (a) Optical, and (b) scanning electron micrographs of a polished and etched surface of the Al_2O_3–SiC composite.

ness [16]. Self-arresting cracks have been grown successfully under compression fatigue in a number of materials: steel and aluminium alloys [15, 18], cemented carbides [19, 20], single-phase polycrystalline alumina, silicon nitride, transformation-toughened ceramics [16, 17], and silicon carbide-reinforced silicon nitride [21]. It is of interest to study the applicability of this technique to toughened ceramics because specimens with pre-cracks grown under compression fatigue are potentially suitable for measuring the fracture toughness as well as the stable crack growth during quasi-static fracture (i.e. *R*-curves).

2. Material and experimental procedures

The SiC whisker-reinforced Al_2O_3 selected for this investigation is the only reinforced ceramic commercially available in the USA (trade name WG-300, The Greenleaf Corp., Saegertown, Pennsylvania). The volume fraction of SiC whiskers was measured to be 33%. The whiskers were 0.2 to 0.7 μm wide and up to 25 μm long, and they tended to be oriented with the longitudinal axis perpendicular to the pressing direction. The microstructural characteristics of these whiskers have been described by Nutt [22, 23]. The average grain size of the Al_2O_3 matrix was 1.3 μm, although whisker-free agglomerates of coarser alumina grains were frequently observed in optical and scanning microscopes (see Fig. 1). Samples of the material were prepared for examination by analytical electron microscopy. Small glass pockets were occasionally observed at triple points formed by grain boundary–interface junctions (Fig. 2). X-ray spectra showed that the glass phase was composed primarily of silicon (and probably oxygen), with trace amounts of potassium, iron, sulphur, calcium, yttrium and molybdenum.

For the crack propagation experiments, notches of different root radii were introduced with diamond wheels in rectangular bars, machined from plates of the composite ceramic. The notches were perpendicular to the axis of the bars, and the root radius varied from 0.13 to 1.05 mm. The specimen surfaces were polished with 15 μm diamond to facilitate the detection of cracks during cyclic loading. Cyclic compressive loads were applied along the axis of the bars, normal to the plane of the notch. The cyclic load was sinusoidal with a frequency of 20 Hz, and the fatigue load ratio, *R*, defined as the ratio of the minimum load to the maximum load, was $R = 10$. The load amplitude was incremented by 10 to 15% for every 20 000 load cycles until the nucleation of a fatigue crack was observed. Then the load was kept constant and the propagation of the crack was monitored with an optical microscope. For the fracture toughness experiments, single and double edge-notched specimens were machined to the nominal dimensions shown in Fig. 3a. A 60° notch with a root radius of 0.15 mm was chosen for these experiments. Fatigue cracks were grown from the notches under uniaxial cyclic

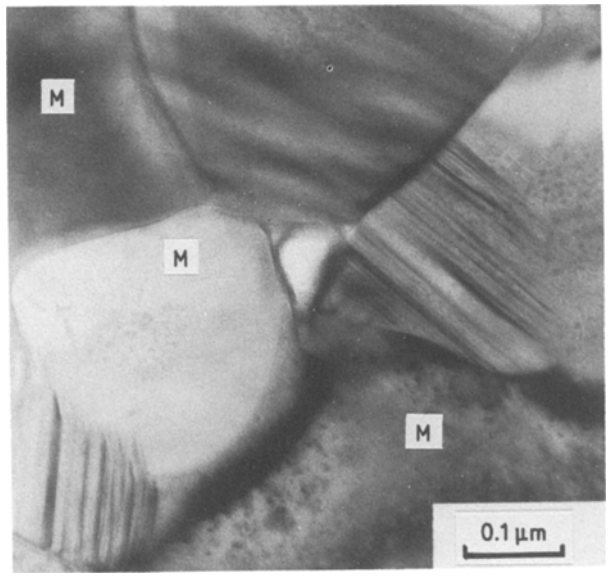

Figure 2 Transmission electron micrograph showing a glass pocket. M indicates matrix grains.

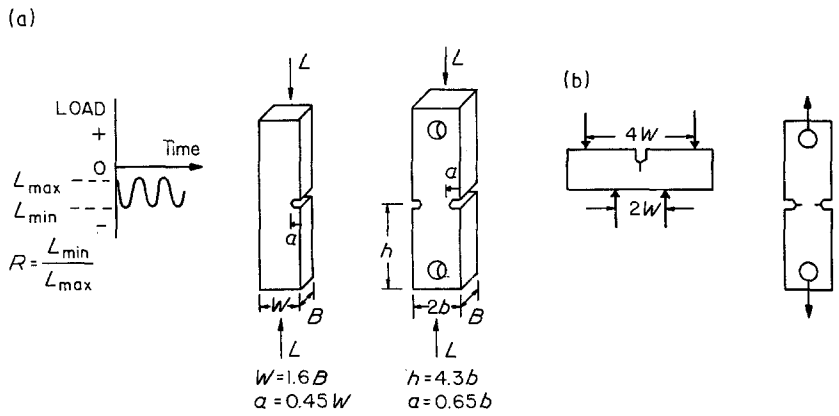

Figure 3 Schematic illustration of the loading configuration for (a) compression fatigue crack initiation and growth in single and double edge-notched specimens, and (b) the corresponding loading for K_{IC} measurement.

compression, with the loading axis perpendicular to the plane of the notch, as shown in Fig. 3a. The cyclic load was of the same form, frequency, and fatigue load ratio as described above. The far-field compressive stress amplitude $|\Delta\sigma|$ was 283 MPa for the single edge-notched specimens, and 386 MPa for the double edge-notched specimens. Cracks nucleated within the first 20 000 load cycles and propagated at decreasing rates for an additional 1 million to 1.5 million cycles before stopping. The final crack length measured on the surface of the specimens was $\sim 200\,\mu m$. After precracking under compressive uniaxial fatigue, the specimens were tested for fracture toughness in four-point bending or in tension, depending on the specimen geometry, as indicated in Fig. 3b. In both cases, the specimens were monotonically loaded to catastrophic fracture in a servo-hydraulic testing machine at a constant cross-head speed of 3×10^{-5} in. sec^{-1} ($\sim 7.6 \times 10^{-5}$ cm sec^{-1}). Using the results of the four-point bend tests, fracture toughness, K_{IC}, was calculated using the equation proposed by Kavishe [24]–

$$K_{IC} = \frac{3P(\pi a)^{1/2}}{BW}\left[1.12 - 1.39\left(\frac{a}{W}\right) + 7.32\left(\frac{a}{W}\right)^2 - 13.1\left(\frac{a}{W}\right)^3 + 14.0\left(\frac{a}{W}\right)^4\right]$$

From the tensile test results, K_{IC} was calculated employing the relation [25]:

$$K_{IC} = \frac{P(\pi a)^{1/2}}{2bB}\left[1 - 0.122\cos^4\frac{\pi a}{2b}\right]\left[\frac{2b}{\pi a}\tan\frac{\pi a}{2b}\right]^{1/2}$$

In both cases, P is the catastrophic fracture load, and a represents the average through-thickness fatigue crack length, which was measured after fracture using an optical microscope. In the above equations, the symbols used denote the following dimensions of the specimens: a = initial crack length (including the notch length); B = thickness of specimen; W = width of single edge-notched specimen; $2b$ = width of double edge-notched specimen; $2h$ = height of double edge-notched specimen (Fig. 3a).

Additional fracture toughness measurements were performed by means of the indentation technique [12]. Two indentations were introduced on each of the three orthogonal surfaces parallel and perpendicular to the pressing direction, as shown in Fig. 4, employing a Vickers indentor. The indentation load was increased monotonically at a rate of 0.05 kg sec^{-1}, up to 10 kg, and held constant for 5 min. The fracture toughness, K_{IC} was calculated using [12]

$$K_{IC} = 0.016\left[\frac{E}{H}\right]^{1/2}\left[\frac{P}{C}\right]^{3/2}$$

where E is the elastic modulus, H is the hardness, P = 10 kg, and C is the length of the crack propagating from the corners of the indentation.

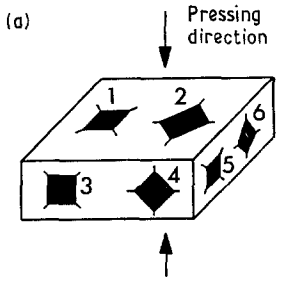

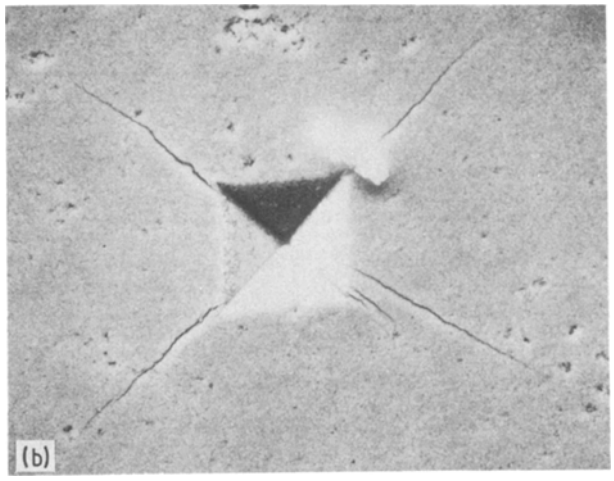

Figure 4 (a) Schematic illustration of the position of the indentations with respect to the pressing direction. (b) SEM picture of radial cracks induced by indentation in SiC whisker-reinforced Al_2O_3.

TABLE I K_{IC} values for precracked specimens (notch root radius = 150 μm)

Specimen	K_{IC} (MPa m$^{1/2}$)	
	Single edge, four-point bending	Double edge, tension
1	5.17	5.12
2	5.26	4.76
3	5.42	
4	5.03	
Average	5.22 ± 0.14	

TABLE II K_{IC} values for single edge-notched specimens without fatigue pre-crack

Notch root (μm)	Specimen	K_{IC} (MPa m$^{1/2}$)
150	1	9.58
	2	8.36
445	3	13.60
	4	12.84

3. Results

3.1. Fracture toughness

Fracture toughness values obtained for single-edge and double-edge notch fatigued specimens with fatigue pre-cracks are listed in Table I. Note that K_{IC} values obtained in four-point bending are reproducible to within ± 0.2 MPa m$^{1/2}$ (or within 3.8%) of the average. The tension test results shown in Table I reflect an underestimate of K_{IC}, because the ratio between the length and the half width of the tension specimens (2.45) is lower than the ratio required to use the present K calibration (2.75, [25]). The required specimen dimensions could not be fully satisfied at the time of these tests because of the limited dimensions of composite plates available from the manufacturer. However, the results of four-point bending and tension are in good agreement and they show that the conventional fracture mechanics approach can be applied to brittle materials that are pre-cracked by compressive fatigue loading.

Table II shows the K_{IC} values obtained from single edge-notched specimens having different notch root radii that were not pre-cracked in compression. These K_{IC} values are less reproducible than those obtained from pre-cracked specimens, and K_{IC} increases with notch root radius.

Results of indentation toughness tests are listed in Table III. The indentation numbers in Table III refer to the poisition and orientation of the indentations with respect to the pressing direction, as shown in Fig. 4a, and the hardness values in that table were calculated using the average length of the indentation diagonals. Four radial cracks were caused by each indentation, and the average crack length, $\bar{a}$, was used to calculate the toughness values shown. The average toughness was 4.12 MPa m$^{1/2}$, and all the values fell within ± 0.48 MPa (or within 12%) of the average. The indentation technique should have been well-suited to the present material, because of the small grain size compared to the size of the indentation, and a chipping threshold (disruption of the radial cracks pattern by lateral cracks) that was far above the 10 kg load employed [12]. In spite of these positive indicators, there were practical difficulties in applying the indentation technique. For example, as shown in the typical indentation of Fig. 4b (see also Fig. 8a in a later section), there was often more than one crack at some corners, and the cracks were not always radial (i.e. parallel to the direction of the indentation diagonals). These geometrical irregularities added uncertainty to the determination of the toughness.

TABLE III K_{IC} values obtained by means of the indentation method. The indentation number refers to Fig. 5 (Vickers indentor, monotonic load, P_{max} = 10 kg)

Indentation number	Hardness (GPa)	Crack length, a (μm)	Average crack length, $\bar{a}$ (μm)	K_{IC}, from $\bar{a}$ (MPa m$^{1/2}$)
1	23.2	117 119 142 124	125	4.60
2	23.1	155 128 157 137	144	3.73
3	22.0	137 124 142 131	134	4.29
4	21.3	150 147 146 131	143	3.93
5	21.1	150 115 139 149	138	4.17
6	20.7	153 124 148 150	144	3.98

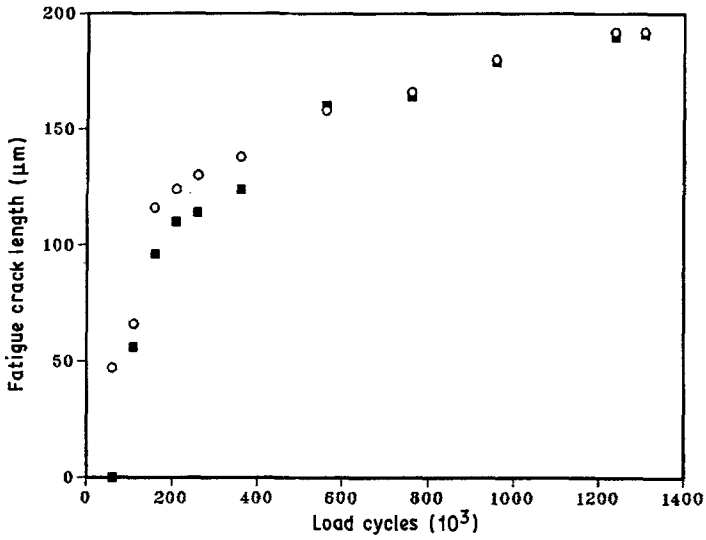

Figure 5 Fatigue crack length as a function of the number of compressive load cycles. The damage induced by surface grinding aids the nucleation and early growth of fatigue cracks: (○) as-received, (■) polished.

3.2. Compression fatigue

The conditions for crack nucleation and growth under compressive cyclic loads were investigated using notched specimens with different notch root radii. For all notches with root radius up to 0.62 mm, the fatigue crack started at the notch and propagated in a plane perpendicular to the loading axis at systematically decreasing rates until it stopped. As the notch root radius was increased, the amplitude of the applied stress intensity factor, $|\Delta K|$, also had to be increased in order to nucleate a crack, and the resulting self-arrested cracks were longer. However, the maximum compressive stress at the notch tip during the applied load cycle, $\sigma_{\theta\theta}$, remained almost independent of the notch root radius. These results are summarized in Table IV. All attempts to initiate a stable Mode I crack under compressive fatigue in specimens with the largest notch root radius (1.05 mm) were unsuccessful.

Additional crack propagation experiments were conducted in order to analyse the effect of surface finish on crack growth. Notched specimens polished only on one side were fatigued in compression, and crack growth was monitored on both the as-received and the polished sides. The crack lengths plotted against the number of fatigue cycles is shown in Fig. 5. The crack appeared first on the unpolished side of the specimen and remained longer than the crack on the polished surface through the initial 6×10^5 load cycles. Grinding marks were visible on the surface of the as-received material when observed with an optical microscope (at $\times 50$). Because damage caused by surface grinding appeared to have an effect on crack nucleation and growth, the nature and extent of that damage was investigated by TEM observations of cross-sectional thin foils. Grinding-induced damage consisted primarily of matrix dislocations and deformation twins, which extended $\sim 10\,\mu m$ below the surface of the as-received material. Fig. 6 shows a representative subsurface grain containing narrow deformation twins which stop at the grain boundary. The twins are ~ 13 nm wide, or 10 lattice constants along the c-axis, and analysis of diffraction patterns indicated that the twin plane was basal. Although twin–twin and twin–grain-boundary interactions in alumina reportedly form microcracks [26], near-surface microcracks were not observed in the as-received composites. However, the damage caused by surface grinding apparently facilitated the nucleation and early growth of fatigue cracks from a sharp notch.

TABLE IV Results of crack propagation under compressive fatigue for different notch root radius (ϱ = notch root radius, a = final crack length, N = total number of load cycles, $|\Delta K|$ = applied stress intensity factor amplitude, $\sigma_{\theta\theta}$ = compressive axial stress at the notch tip)

ϱ (μm)	$\lvert\Delta K\rvert$ (MPa m$^{1/2}$)	$-\sigma_{\theta\theta}$ (MPa)	a (μm)	N (10^6 cycles)
130	74.8	8223	182	1.16
150	82.3	8424	200	1.5
174	82.3	7799	262	1.08
375	113.3	7334	251	1.00
620	150.7	7587	835	1.11
1050	No crack growth, catastrophic failure			

4. Discussion

4.1. Fracture behaviour

The measured fracture toughness of pre-cracked specimens of SiC whisker-reinforced Al_2O_3 represents an

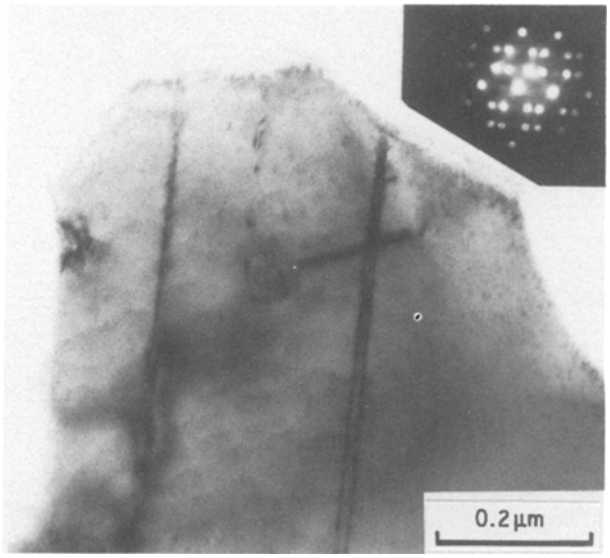

Figure 6 Twins formed by grinding in a near-surface matrix grain. The spot pattern in the insert shows the superposition of the matrix and twin spots (basal twin, B = [1 2 1 0]).

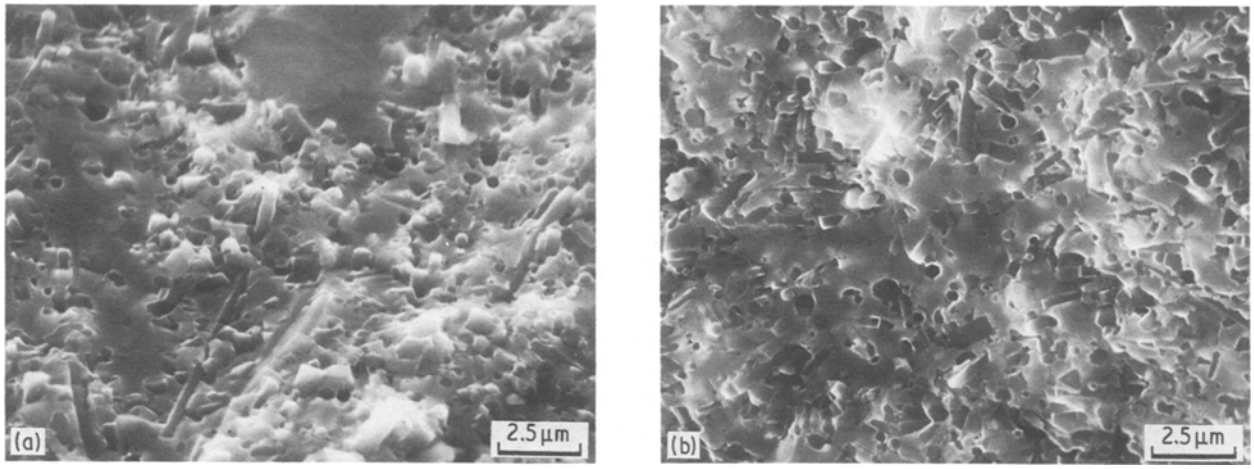

Figure 7 Scanning electron micrographs (a) of the fatigue crack surface (notice the flattening produced on some regions as a result of repeated surface contact), and (b) of the catastrophic fracture surface.

increase compared to the toughness of unreinforced Al_2O_3. Suresh *et al.* [21] employed the four-point bend configuration on pre-cracked specimens of high-purity Al_2O_3 with a grain size from 1 to 6 μm. They obtained an average toughness of 3.45 MPa $m^{1/2}$. Employing cylindrical rods of high-purity Al_2O_3 with a grain size of 1 to 3 μm, pre-cracked in compression, Tschegg and Suresh [17] measured the fracture toughness in tension. They obtained an average toughness of 3.35 MPa $m^{1/2}$, in excellent agreement with the results of four-point bend tests [16]. Based on these reports and the results shown in Table I, the SiC whisker-reinforcement improves the toughness by 50%. The values of toughness measured with the indentation technique are consistent with this observation. Porter *et al.* [4] applied the indentation technique to fine-grained Al_2O_3 and SiC whisker-reinforced Al_2O_3. As in the present measurements, they used a Vickers indentor and a 10 kg load. They obtained toughness values of 2.1 MPa $m^{1/2}$ for the unreinforced material, and 3.6 and 4.6 MPa $m^{1/2}$ in Al_2O_3 reinforced with 5 and 15% volume fraction of SiC whiskers, respectively. The latter value is in good agreement with the values in Table III for material with 33% volume fraction of SiC whiskers. Bend tests on notched bars without pre-cracks resulted in considerably higher and less reproducible toughness values, as shown in Table II. These values are similar to those obtained from short rods of Al_2O_3 reinforced with 20 and 30% SiC whiskers [1].

Inspection of the fracture surface in the scanning electron microscope (SEM) shows that the mode of failure is mostly interfacial and intergranular, Fig. 7. Some cleavage steps were occasionally observed in the matrix grains, as reported previously on unreinforced Al_2O_3 [16]. The matrix in the composite appears to fail like the unreinforced Al_2O_3. Although whisker debonding, whisker pullout, and through-whisker fracture were apparent in the composite, it is difficult to determine a toughening mechanism from this evidence. If a crack-bridging mechanism were the main toughening process, it would be apparent when observing a surface of the composite normal to the plane of the crack. The radial cracks emanating from the corners of the indentation were suitable for this kind of observation. However, as shown in Figs 8b and c, even in this case insufficient evidence was found to support a crack-bridging mechanism of toughening.

4.2. Toughness testing techniques

To date, none of the procedures reported in the literature for measuring fracture toughness of brittle solids have been adopted as a standard. The reason for a lack of a standard is that some of these methods depend on geometrical factors, while others can be used only on some materials. There are indications that the results obtained using the notched bar, the chevron notch, and the bridge compression configurations are affected by the geometry of the notch and/or the specimen dimensions [7, 8, 10, 13, 14]. On the other hand, the crack measurements involved in the indentation method can be a source of substantial error, and the method is not applicable to brittle materials which present multiple cracking or crack branching during indentation [12]. Although indentations are a simple means to introduce stable cracks in some brittle solids, the actual extent of cracking cannot be detected in opaque materials, and the residual plastic deformation developed around the indentation can severely affect subsequent fracture toughness measurements. Furthermore, when comparing toughness results from different sources, care should be taken that the same load and equations are used to evaluate K_{IC}.

The results on SiC whisker-reinforced Al_2O_3 listed in Table II show that the toughness values obtained with the notched bend bar depend on the root radius of the notch. As the notch root radius is increased, the toughness values increase and the results are less consistent. The results in Table III, obtained by the indentation technique, are more reproducible than those obtained with the notched specimens. However, it was difficult to determine accurately the length of the cracks, and the application of the indentation technique to this composite is questionable because multiple cracking occurred at some indentation corners (Fig. 8a).

The most reproducible toughness values were obtained using pre-cracked specimens. Also, the

agreement between single and double edge-notched specimen results of Table I indicates that pre-cracking in compression enables the use of different geometries with well-established stress intensity factor calibrations. Although in some materials it may be difficult to measure accurately the fatigue crack length, this length is small compared to the notch depth, and the resulting error in the value of K_{IC} is small, because the length involved in calculating K_{IC} is the total length of the notch plus the fatigue crack. Furthermore, specimens pre-cracked under compression fatigue are suitable to obtain crack resistance curves by the same procedures used here to measure toughness. However, R-curves were not obtained at the same time of the toughness tests because the testing machine employed was not rigid enough for such measurements. A possible limitation of the technique is that it can be applied only to those materials on which stable cracks can be grown in compression. So far, however, all attempts to grow fatigue cracks using compressive cyclic loads in brittle solids have been successful, except in single crystals of ceramics and in glass [16, 19–21].

4.3. Behaviour in compression fatigue

Crack growth in SiC whisker-reinforced Al_2O_3 by compressive fatigue is analogous to the crack growth reported for unreinforced Al_2O_3 [16], i.e. the crack starts at the notch and propagates perpendicular to the loading direction at decreasing rates until it arrests. Another characteristic feature of compression fatigue crack growth observed previously is the formation of debris behind the crack tip [16]. The debris formed during fatigue results in two main effects. First, near the free surface of the specimen the debris falls off, leaving an open crack that can grow faster and longer than a sharp crack that closes during part of the loading cycle. Secondly, behind the crack tip in the interior of the specimen, the debris, and the pulled out whiskers, trapped between the crack surfaces provide additional contact forces. These forces act as a closure mechanism slowing the fatigue crack growth. Thus, the generation and loss of debris particles causes the crack to be longer along the free surface than in the interior of the specimen. Inspection of the fracture surface showed that the average fatigue crack length decreased, within a layer of about 65 μm, from 200 μm on the surface to a uniform length of 100 μm in the interior of the specimen. Ewart and Suresh [16] observed a similarly shaped crack front in Al_2O_3 subjected to compressive fatigue. Also, their experiments proved that removal of the debris formed behind the crack tip in Al_2O_3 resulted in longer and faster growing cracks. Note that loss of debris from notch ends during fatigue is more severe in the composite than in the unreinforced alumina. It has been observed in SiC whisker-reinforced Si_3N_4 that crumbling increases with increasing volume fraction of whiskers [21]. Thus, SiC whisker reinforcement appears to contribute to an increase in the apparent crack opening displacement during fracture under far-field cyclic compression.

The length of the self-arrested fatigue crack increases with the notch root radius (Table IV). In all cases, the cracks grown by compressive fatigue in SiC whisker-reinforced Al_2O_3 are somewhat shorter than those reported in the literature for other brittle materials. Ewart and Suresh [16] obtained cracks of 1 to 2 mm in alumina specimens with a notch root radius of 0.70 mm, and Sylva and Suresh [19] reported crack lengths of 0.6 to 1.2 mm in cemented WC specimens with notch root radius 0.50 mm. However, the length of the self-arrested cracks cannot be attributed solely to the

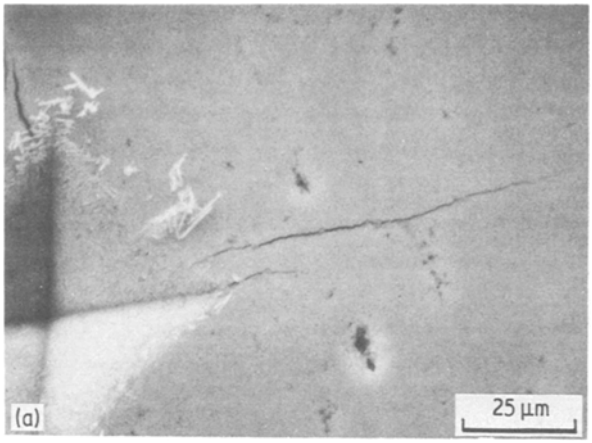

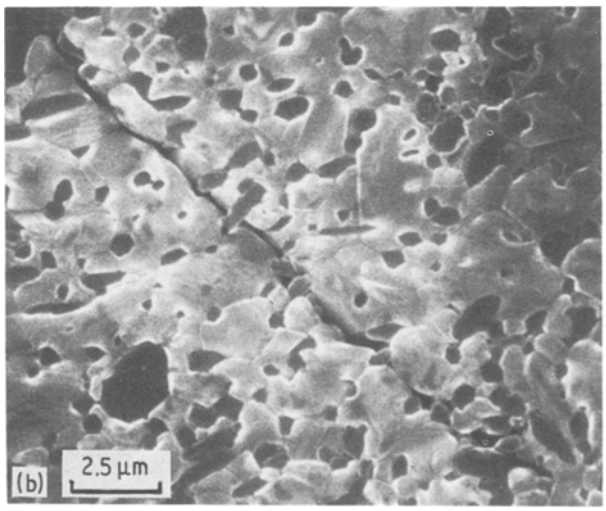

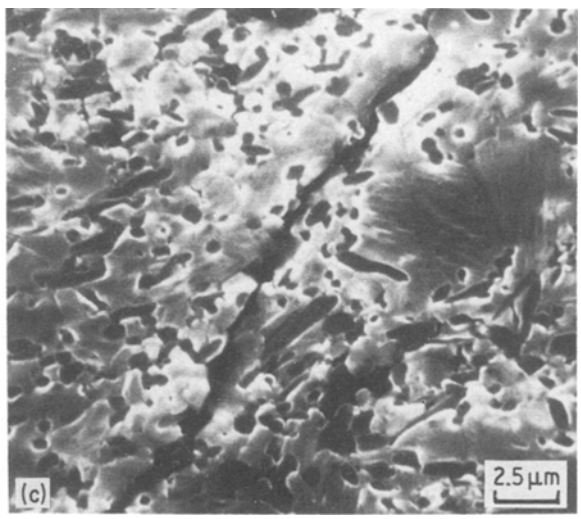

Figure 8 (a) Multiple cracking and crack branching frequently induced by indentation cracking in the Al_2O_3–SiC composite. (b) and (c) Some instances of crack bridging and deflection were observed.

difference in specimen material. Other variables may be correlated to the length of the arrested fatigue crack in addition to the notch root radius. For example, in alloy steels, a larger compressive fatigue load amplitude produced longer cracks until a maximum (load independent) crack length was achieved for the same notch geometry [27]. The results shown in Table IV were obtained increasing the load in 10% to 15% increments, until a crack started to grow. Experimental results on fatigue crack growth on ceramics are still needed to determine the dependence of the self-arrested crack length on load amplitude and notch geometry.

The failure to initiate a crack using the 1.05 mm notch root radius indicates that the notch geometry for crack initiation under compressive fatigue is limited to narrow notches with sharp radii. However, in the case of the large notch, a crack initiated elsewhere under compression fatigue leading to failure. These observations, and the ease with which cracks were grown from sharp notches, indicate that in spite of the high compressive strength of ceramics, and ceramic composites, variable compressive loads may cause crack nucleation from internal defects and stress concentrations, which can lead to premature failure.

5. Summary and Conclusions

Results of fracture toughness measurements and compressive fatigue crack growth experiments on an Al_2O_3–SiC composite have been presented. The results show that:

1. Specimens of SiC whisker-reinforced Al_2O_3 pre-cracked by compressive cyclic loads gave consistent toughness values that represent a 60% increase in toughness compared to unreinforced Al_2O_3. Although whisker pull-out, crack bridging, and crack deflection were observed, none of these could be singled out as the primary toughening mechanism.

2. Toughness values obtained from bend and tensile tests on pre-cracked specimens showed good agreement. However, K_{IC} values obtained from notched bars without pre-cracks were 70 to 150% higher, depending on the notch root radius.

3. Pre-cracking using compression fatigue enables the use of the fracture mechanics approach established for metals. The technique is applicable to a wider range of brittle materials than other methods presently being used. The proper $|\Delta K|$ to initiate a crack is easily determined, and consistent K_{IC} values can be obtained provided the initial notch is sharp (for the materials studied to date, a notch root radius $\leqslant 0.7$ mm).

4. Under compressive cyclic loads, cracks nucleated from sharp notches and propagated at decreasing speeds before arresting. Although ceramic composites are much stronger in compression than in tension, and present attractive possibilities for compression-dominated applications, they exhibit stable, subcritical, fatigue crack growth at room temperature under cyclic compressive loads.

Acknowledgements

This research was supported by the Brown University MRG under contract no. DMR-8714665. The authors are grateful for the assistance received at the Central Facilities for Mechanical Testing and Microscopy at Brown University, and for the use of their equipment.

References

1. G. C. WEI and P. F. BECHER, *Amer. Ceram. Soc. Bull.* **64** (1985) 298.
2. P. F. BECHER and G. C. WEI, *J. Amer. Ceram. Soc.* **67** (1984) C-267.
3. J. HOMENY, W. L. VAUGHN and M. K. FERBER, *Amer. Ceram. Soc. Bull.* **66** (1987) 333.
4. J. R. PORTER, F. F. LANGE and A. H. CHOKSHI, *ibid.* **66** (1987) 343.
5. M. V. SWAIN and R. H. J. HANNINK, in "Advances in Ceramics", Vol. 12, edited by N. Claussen, M. Ruhle and A. H. Heuer (American Ceramic Society, Columbus, Ohio, 1984) pp. 225–232.
6. R. KREHANS and R. STEINBRECH, *J. Mater. Sci. Lett.* **1** (1982) 327.
7. L. M. BARKER, *Eng. Fract. Mech.* **9** (1977) 361.
8. D. MUNZ, R. T. BUBSEY and J. E. SRAWLEY, *Int. J. Fract.* **16** (1980) 359.
9. T. SADAHIRO and S. TAKATSU, *Mod. Div. Powder Metall.* **14** (1980) 561.
10. R. WARREN and B. JOHANNESSON, *Powder Metall.* **27** (1984) 25.
11. A. G. EVANS and T. R. WILSHAW, *Acta Metall.* **24** (1976) 939.
12. G. R. ANSTIS, P. CHANTIKUL, B. R. LAWN and D. B. MARSHALL, *J. Amer. Ceram. Soc.* **64** (1981) 533.
13. J. L. SHANNON Jr and D. G. MUNZ, in "Chevron-Notched Specimens: Testing and Stress Analysis", ASTM STP 855 edited by J. H. Underwood, S. W. Freiman and F. I. Baratta (American Society for Testing and Materials, Philadelphia, 1984) pp. 270–80.
14. A. R. INGRAFFEA, K. L. GUNSALLUS, J. F. BEECH and P. P. NELSON, "A Short-Rod Based System for Fracture Toughness Testing of Rock", ASTM STP 855 edited by J. H. Underwood, S. W. Freiman and F. I. Baratta (American Society for Testing and Materials, Philadelphia, 1984) pp. 152–166.
15. S. SURESH, T. CHRISTMAN and C. BULL, Crack Initiation and Growth Under Far Field Cyclic Compression: Theory, Experiments and Applications, in "Small Fatigue Cracks", edited by R. O. Ritchie and J. Lankford (The Metallurgical Society of AIME, Warrendale, Pennsylvania, 1986) pp. 513–40.
16. L. EWART and S. SURESH, *J. Mater. Sci.* **22** (1987) 1173.
17. E. K. TSCHEGG and S. SURESH, *J. Amer. Ceram. Soc.* **70** (1987) C-41.
18. R. P. HUBBARD, *J. Basic Engng Trans. ASME* **91** (1969) 625.
19. L. A. SYLVA and S. SURESH, *Mater. Sci. Engng* **83** (1986) L7.
20. R. GODSE, J. GURLAND and S. SURESH, "Crack Growth Under Far Field Cyclic Compression in Hardmetals", presented at the TMS meeting, Denver, Colorado, February 1987.
21. S. SURESH, L. X. HAN and J. J. PETROVIC, *J. Amer. Ceram. Soc.* **71** (1988) C158.
22. S. R. NUTT, *ibid.* **71** (1988) 149.
23. *Idem, ibid.* **67** (1984) 428.
24. F. P. L. KAVISHE, *Int. J. Fract.* **27** (1985) R13.
25. H. TADA, P. C. PARIS and G. IRWIN, "The Stress Analysis of Cracks Handbook" (Del Research Corp., Hellertown, Pennsylvania, 1973).
26. A. H. HEUER, *Phil. Mag. A* **13** (1986) 379.
27. S. SURESH, *Engng Fract. Mech.* **21** (1985) 453.

Received 24 August
and accepted 1 December 1987